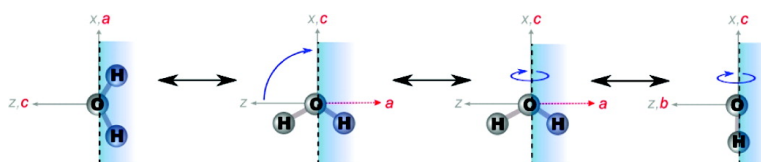


Water at Hydrophobic Surfaces: When Weaker Is Better

Dennis K. Hore, Dave S. Walker, and Geraldine L. Richmond

J. Am. Chem. Soc., **2008**, 130 (6), 1800-1801 • DOI: 10.1021/ja0755616

Downloaded from <http://pubs.acs.org> on February 8, 2009



More About This Article

Additional resources and features associated with this article are available within the HTML version:

- Supporting Information
- Links to the 4 articles that cite this article, as of the time of this article download
- Access to high resolution figures
- Links to articles and content related to this article
- Copyright permission to reproduce figures and/or text from this article

[View the Full Text HTML](#)

Water at Hydrophobic Surfaces: When Weaker Is Better

Dennis K. Hore,[†] Dave S. Walker,[§] and Geraldine L. Richmond*

Department of Chemistry, University of Oregon, Eugene, Oregon 97403

Received July 25, 2007; E-mail: richmond@uoregon.edu

The upsurge of interest in the nature of water adjacent to hydrophobic liquids is due in part to the growing appreciation for its unique characteristics for supporting chemical synthesis, nano-particle assembly, oil remediation, and a host of other chemical separation processes.^{1,2} The important characteristics of these interfaces that lend themselves to these applications—molecular orientation, polarity, interfacial charge and electric fields—all stem from the disruption of the bulk water hydrogen-bonding network.^{3–5} Water molecules seem to adapt to hydrophobic neighbors by rearranging themselves to maximize available hydrogen-bonding opportunities and minimize unfavorable dipole interactions.⁶ Using equilibrium molecular dynamics simulations, we have discovered that this adaptation follows trends associated with the molecular properties of the hydrophobic liquid neighbor. Our studies reveal that the degree of water structuring in the immediate vicinity of the oil–water junction is highest when the hydrophobic phase is the least polar, that polar organics result in wider interfacial regions, and that the maximum extent of water molecule orientation does not occur at the Gibbs dividing surface.

We have used the Amber 7 package⁷ to perform the molecular dynamics simulations. A cubic box, 40 Å on each side and containing 2135 POL3⁷ water molecules, was minimized and equilibrated for 200 ps. Temperature was controlled by weak coupling to a heat bath at 300 K; molecular geometries were constrained using the SHAKE algorithm; long-range interactions were limited to 8 Å using the particle mesh Ewald technique. A separate box the same size was prepared, either empty (to simulate the air–water interface) or with carbon tetrachloride, dichloromethane, or chloroform. The organic models and associated point charges were taken from the literature.^{8–11} The number of organic molecules (Table 1) was selected to reproduce the bulk densities of the liquids at room temperature. The hydrophobic liquids were minimized and equilibrated in a similar fashion to the bulk water box. Hydrophobic–aqueous interfaces were then prepared by joining an equilibrated water box with an equilibrated hydrophobic box to create a 40 × 40 × 80 Å³ system that was then subject to further energy minimization and equilibration. The dynamics of each system were then followed for 10 ns, and we recorded atomic coordinates every 50 fs. The results we describe are therefore based on ensemble averages of 200 000 configurations for each system. Density profiles from the simulations were fit to a hyperbolic tangent profile (solid lines in Figure 1) to obtain the position of the Gibbs dividing surface. For all subsequent analyses, care was taken to align the Gibbs surfaces for each aqueous–hydrophobic system studied.

Order parameters^{2,12–14} are formulated as a measure of the extent to which the water molecules tend to orient with respect to the lab frame coordinates (Figure 2). The parameter $S_1 = 0.5(3 \cos^2 \theta - 1)$ quantitatively describes the degree of ordering of the tilt angle,

Table 1. Interfacial Widths and Some Other Parameters Associated with the Hydrophobic Phase in Contact with Water^a

organic molecule	density (g mL ⁻¹)	molecules (40 Å) ³	dipole moment (D)	interfacial width (Å)	"90–10" equiv width (Å)
none (air)	0	0	N/A	1.96	4.31
CCl ₄	1.6	400	0.00	2.08	4.56
CHCl ₃	1.5	475	1.14	2.27	5.00
CH ₂ Cl ₂	1.3	601	1.83	3.31	7.27

^a Bulk liquid dipole moments come from the chloroform^{8,10} and dichloromethane^{9,11} models. The interfacial width was determined by fitting the molecular dynamics coordinate data to a hyperbolic tangent profile.

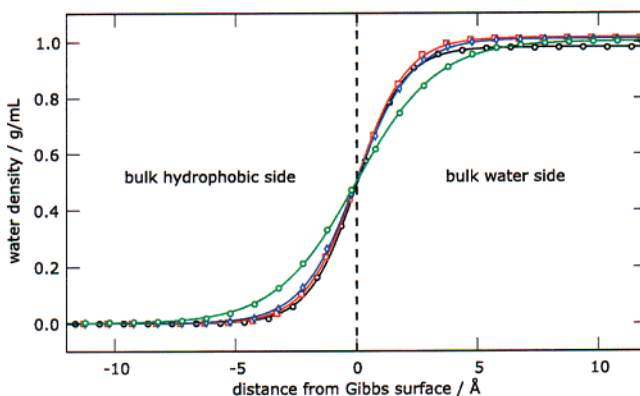


Figure 1. Density of water molecules across various hydrophobic interfaces. Air–water (black), carbon tetrachloride–water (red), chloroform–water (blue), and dichloromethane–water (green). The abscissa have been calibrated so the Gibbs dividing surfaces ($z = 0$) are aligned for all systems.

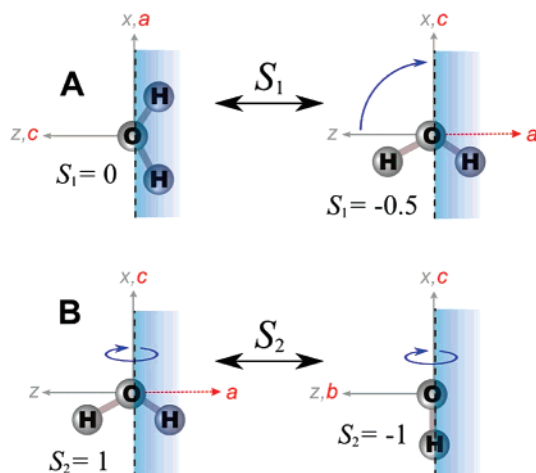


Figure 2. Order parameters useful for describing the extent to which water molecules are structured at the hydrophobic–aqueous interface. (a) The tilt order parameter S_1 describes the extent to which the molecular c -axes are ordered with respect to the interface normal, z . (b) The twist order parameter S_2 describes the extent to which the water molecules are twisted about their c -axes.

[†] Present address: Department of Chemistry, University of Victoria, Victoria, British Columbia, V8W 3V6, Canada.

[§] Present address: TriQuint Semiconductor, Inc., Hillsboro, Oregon, 97124.

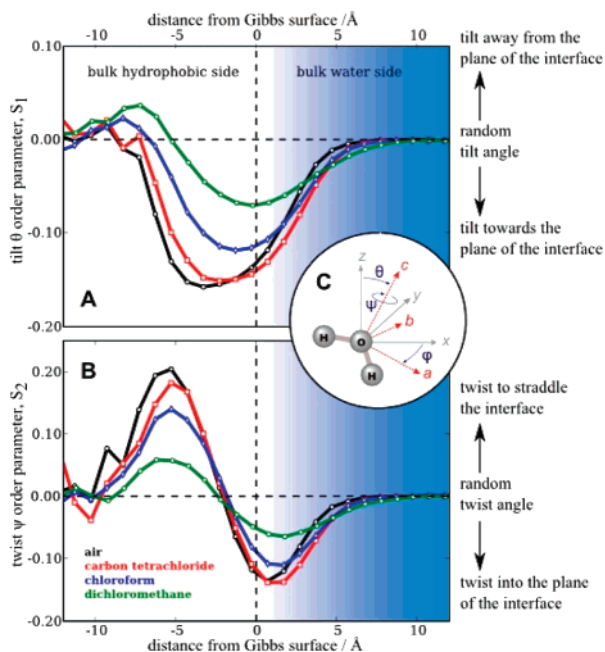


Figure 3. Water molecules next to four hydrophobic phases. (a) Tilt order parameter for water molecules at the interface with air (black), carbon tetrachloride (red), chloroform (blue), and dichloromethane (green) as a function of distance from the Gibbs surface. Positive values of the distance are toward the bulk water phase. All values are normalized to the number of water molecules found at that location. (b) Twist order parameter for the same systems. (c) Definition of tilt and twist angles that describe the orientation of water molecules with respect to the interfaces.

θ , between the water c -axes and the interface normal, z (Figure 2a). Within the range $-0.5 < S_1 < 1$, a value of $S_1 = 1$ represents water molecules perfectly aligned with their c -axes sticking out of the surface, whereas $S_1 = -0.5$ represents perfect alignment with the c -axes in the plane of the surface. A second parameter, $S_2 = \langle \sin \theta \cos 2\psi \rangle / \langle \sin \theta \rangle$, measures the degree to which the molecules are twisted by ψ about their c -axes (Figure 2b). The range for this order parameters is $-1 < S_2 < 1$. The extreme $S_2 = 1$ represents a twist of the molecular axes to perfect alignment with $\phi = 0^\circ$ or 180° ; $S_2 = -1$ indicates $\phi = 90^\circ$ or 270° . (An isotropic/bulk distribution would have both order parameters equal to zero.)

Given that the *magnitude* of the order parameters reflect the degree of molecular orientation, Figure 3, panels a and b clearly indicate that organic liquids with weaker dipole moments encourage a greater orientation of water molecules near the Gibbs dividing surface. Interestingly, this trend reverses for the small number of water molecules found at the extreme end of the interfacial oil phase, where the alignment has the oxygen atoms directed toward the bulk water phase (Figure 3a). This can be seen as $S_1 > 0$ in Figure 3a and has been the subject of a detailed investigation in this laboratory.⁶ We also find that organics with stronger dipole moments result in wider interfacial regions (Figure 1 and Table 1), in agreement with what has been observed experimentally.^{15,16} It is of interest to note that the maxima in water orientation are not peaked at the Gibbs dividing surfaces.

When the two order parameters are viewed together, two dominant orientations of interfacial water molecules are found: those “straddling” the interface with one OH bond directed toward the bulk water phase and the other toward the bulk hydrophobic phase, and those with both OH bonds oriented in the plane of the

interface. These species may be easily distinguished by the sign of the twist order parameter in Figure 3b with $S_2 > 0$ for straddling waters and $S_2 < 0$ for in-plane waters. The straddling water molecules show their maximum order in the organic phase at a distance of 6 Å from the Gibbs surface, whereas the in-plane water molecules show maximum orientation 1 Å into the water side of the interface. Although this twist-order behavior producing straddling (hydrophobic side) and in-plane (aqueous side) orientation is present for all systems, the trend in the *extent* of the ordering follows that of the orientation near the Gibbs surface: hydrophobic phases with weaker dipole moments promote greater structuring of interfacial water molecules.

A recent nonlinear vibrational spectroscopic study monitored water OH stretching modes as an indicator of the strength of hydrogen-bonding next to various halocarbon interfaces.¹⁷ That studied concluded that a stronger water–organic interaction induces a weaker structuring of interfacial water molecules.

We have demonstrated that for hydrophobic–aqueous interfaces, particularly those of industrially and environmentally important chlorinated organic liquids, hydrophobic phases with large dipole moments do not necessarily promote strong ordering of adjacent water molecules; in fact the opposite trend is generally observed. Furthermore, this same trend is observed in the width of the order parameters as they span the interfacial region. Finally, the maxima in water orientation are not peaked at the Gibbs dividing surfaces. Water structure at hydrophobic interfaces is a complex and multifaceted phenomenon that depends on characteristics such as charge, dielectric constant, and molecular shape/geometry in addition to dipole moment. Knowledge of these subtle interactions will lead to an increased understanding of water structure in the presence of ions, surfactants, and biological interfaces.

Acknowledgment. We gratefully acknowledge support for this study from the National Science Foundation (Grant CHE-0652531). We thank Cathryn McFearnin for valuable discussions.

Supporting Information Available: Complete reference 7. This material is available free of charge via the Internet at <http://pubs.acs.org>.

References

- (1) Chandler, D. *Nature* **2007**, *445*, 831–832.
- (2) Jedlovsky, P.; Vincze, A.; Horvai, G. *J. Mol. Liq.* **2004**, *109*, 99–108.
- (3) Benjamin, I. *J. Phys. Chem. B* **2005**, *109*, 13711–13715.
- (4) Du, Q.; Superfine, R.; Freysz, E.; Shen, Y. R. *Phys. Rev. Lett.* **1993**, *70*, 2313–2316.
- (5) Luo, G.; Malkova, S.; Pingali, S. V.; Schultz, D. G.; Lin, B.; Meron, M.; Benjamin, I.; Vanysek, P.; Schlossman, M. L. *J. Phys. Chem. B* **2006**, *110*, 4527–4530.
- (6) Hore, D. K.; Walker, D. S.; MacKinnon, L.; Richmond, G. L. *J. Phys. Chem. C* **2007**, *111*, 8832–8842.
- (7) Case, D. A. et al. *Amber 7*; University of California: San Francisco, CA, 2002.
- (8) Chang, T. M.; Dang, L. X. *J. Phys. Chem. B* **1997**, *101*, 10518–10526.
- (9) Dang, L. X. *J. Phys. Chem. B* **2001**, *105*, 804–809.
- (10) Chang, T.-M.; Dang, L. X.; Peterson, K. A. *J. Phys. Chem. B* **1997**, *101*, 3413–3419.
- (11) Dang, L. X. *J. Chem. Phys.* **1999**, *110*, 10113–10122.
- (12) Buffeteau, T.; Lagugne Labarthe, F.; Sourisseau, C.; Kostromine, S.; Bieringer, T. *Macromolecules* **2004**, *37*, 2880–2889.
- (13) Straley, J. P. *Phys. Rev. A* **1974**, *10*, 1881–1887.
- (14) Photinos, D. J.; Bos, P. J.; Doane, J. W.; Neubert, M. E. *Phys. Rev. A* **1979**, *20*, 2203–2211.
- (15) Walker, D. S.; Brown, M. G.; McFearnin, C. L.; Richmond, G. L. *J. Phys. Chem. B* **2004**, *108*, 2111–2114.
- (16) Scatena, L. F.; Richmond, G. L. *Science* **2001**, *292*, 908–912.
- (17) McFearnin, C. L.; Richmond, G. L. *J. Mol. Liq.* **2007**, *136*, 221–226.

JA0755616